J|A|C|S
ARTICLES
Published on Web 12/30/2003

Modeling the Structure of Amorphous MoS_3: A Neutron Diffraction and Reverse Monte Carlo Study

Simon J. Hibble* and Glenn B. Wood

Contribution from the School of Chemistry, University of Reading, Reading RG6 6AD, U.K.

Received July 31, 2003; E-mail: s.j.hibble@rdg.ac.uk

Abstract: A model for the structure of amorphous molybdenum trisulfide, *a*-MoS_3, has been created using reverse Monte Carlo methods. This model, which consists of chains of MoS_6 units sharing three sulfurs with each of its two neighbors and forming alternate long, nonbonded, and short, bonded, Mo−Mo separations, is a good fit to the neutron diffraction data and is chemically and physically realistic. The paper identifies the limitations of previous models based on Mo_3 triangular clusters in accounting for the available experimental data.

Introduction

Molybdenum trisulfide has been widely studied because of its possible role in hydrodesulfurization catalysts[1] and as an intermediate in the formation of such catalysts from oxide and sulfide precursors.[2,3] This interest coupled with a fundamental interest in "simple" binary sulfides has resulted in a number of attempts, both experimental and theoretical, to determine the structure of MoS_3.[1,4−14] This is not a straightforward procedure because molybdenum trisulfide has never been prepared in a crystalline form, but is always amorphous.

Determining the structure of amorphous solids presents difficulties of both a practical and conceptual nature. The absence of translational symmetry means that a complete description of the structure of an amorphous material requires the position of every atom to be determined. This is impossible, but fortunately it is still possible to obtain meaningful structural information from amorphous materials and to produce realistic three-dimensional models. How we have achieved this in the case of *a*-MoS_3 is described below.

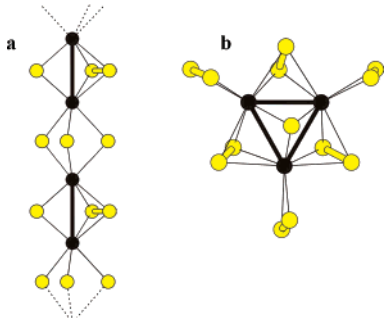

Figure 1. (a) Possible chain model for MoS_3, with S−S bond in alternate S_3 links, resulting in the formula $Mo^{V}(S^{2-})_2(S_2^{2-})_{1/2}$, and (b) the Mo_3S_{13} unit suggested as a structural building block for amorphous MoS_3 (solid circles Mo, yellow circles S, dashed lines indicate bonds to further atoms in the infinite chain).

In the case of *a*-MoS_3 there is a body of experimental measurements from EXAFS,[4−7] X-ray[8,9] and neutron diffraction,[10] photoelectron spectroscopy (PES),[1,4,8] infrared spectroscopy,[1,4,11] and chemical excision,[1,7,12,13] which have been taken along with chemical intuition to produce a range of structural models for the units present. The models proposed include the chain model,[4,8] built from octahedral MoS_6 units sharing opposite triangular faces, Figure 1a, models containing linked Mo_3 triangular clusters,[12] and isolated Mo_3 clusters.[14] The chain model is the simplest conceptually and leads naturally to the correct composition, since every sulfur is bonded to two molybdenum atoms ($MoS_{6/2} \equiv MoS_3$). Recently, models built from Mo_3 triangular clusters have been more popular.[1,7,10,12,14] This is probably due in part to the fact that many molybdenum sulfide clusters containing metal−metal bonded Mo^{IV} triangles are known. For example, the $Mo^{IV}{}_3S_{13}{}^{2-}$ ion shown in Figure 1b is found in $[NH_4]_2[Mo_3S_{13}]$.[15]

Weber et al.[1] claimed that photoelectron spectroscopy showed that all the molybdenum in MoS_3 is Mo^{IV} and that infrared spectroscopy demonstrated that MoS_3 contained at least some

(1) Weber, T.; Muijsers, J. C.; Niemantsverdriet, J. W. *J. Phys. Chem.* **1995**, *99*, 9194, and references therein.
(2) Prins, R.; De Beer, V. H. J.; Somorjai, G. A. *Catal. Rev.-Sci. Eng.* **1989**, *31*, 1.
(3) De Jong, A. M.; Borg, H. J.; van IJzendoorn, L. J.; Soudant, V. G. F. M.; de Beer, V. H. J.; van Veen, J. A. R.; Niemantsverdriet, J. W. *J. Phys. Chem.* **1993**, *97*, 6477.
(4) Liang, K. S.; Cramer, S. P.; Johnston, D. C.; Chang, C. H.; Jacobson, A. J.; deNeufville, J. P.; Chianelli, R. R. *J. Noncryst. Sol.* **1980**, *42*, 345.
(5) Cramer, S. P.; Liang, K. S.; Jacobson, A. J.; Chang, C. H.; Chianelli, R. R. *J. Am. Chem. Soc.* **1984**, *23*, 1215.
(6) Hibble, S. J.; Rice, D. A.; Pickup, D. M.; Beer, M. P. *Inorg. Chem.* **1995**, *34*, 5109.
(7) Hibble, S. J.; Feaviour, M. R.; Almond, M. J. *J. Chem. Soc., Dalton Trans.* **2001**, 935.
(8) Liang, K. S.; deNeufville, J. P.; Jacobson, A. J.; Chianelli, R. R. *J. Noncryst. Sol.* **1980**, *35* and *36*, 1249.
(9) Chien, F. Z.; Moss, S. C.; Liang, K. S.; Chianelli, R. R. *Phys. Rev. B* **1984**, *29*, 4606.
(10) Hibble, S. J.; Walton, R. I.; Pickup, D. M.; Hannon, A. C. *J. Noncryst. Sol.* **1998**, *232−234*, 434.
(11) Chang, C. H.; Chan, S. S. *J. Catal.* **1981**, *72*, 139.
(12) Müller, A.; Fedin, V.; Hegetschweiler, K.; Amrein, W. *J. Chem. Soc., Chem. Commun.* **1992**, 1795.
(13) Müller, A.; Diemann, E.; Krickmeyer, E.; Walberg, H.-J.; Bögge, H.; Armatage, A. *Eur. J. Solid State Chem.* **1993**, *30*, 565.
(14) Jiao, H.; Li, Y.; Delmon, B.; Halet, J. *J. Am. Chem. Soc.* **2001**, *123*, 7334.
(15) Müller, A.; Sarkar, S.; Bhattacharyya, R. G.; Pohl, S.; Dartmann, M. *Angew. Chem., Int. Ed. Engl.* **1978**, *17*, 535.

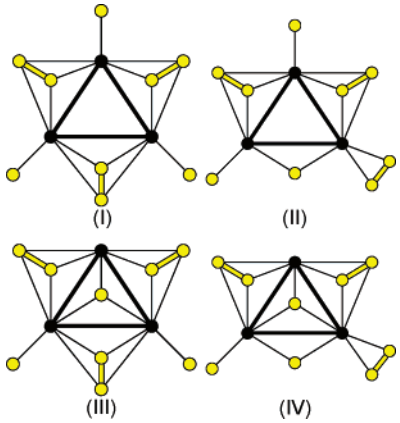

Figure 2. Possible Mo_3S_9 (solid circles Mo, yellow circles S) building blocks (after Weber et al.[1]).

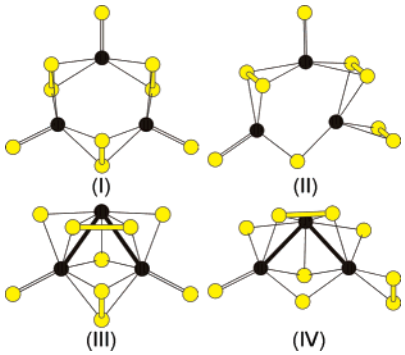

Figure 3. Energy-minimized isolated Mo_3S_9 clusters (solid circles Mo, yellow circles S) of Jiao et al.[14]

units containing the central triply bonding apical sulfur found in the $Mo_3S_{13}^{2-}$ ion. However, there are difficulties in using the Mo_3S_{13} unit as a structural unit because, due to the presence of the triply bridging central sulfur atom, it is impossible to arrive at the composition MoS_3 using this unit alone. Weber et al.[1] suggested that MoS_3 is made up of four different cluster types linked together. These clusters are shown in Figure 2.

Each of the cluster types Weber et al.[1] proposed has the stoichiometry Mo_3S_9. However, Weber et al.[1] did not envisage that these cluster types existed as isolated units, but that they were linked together by sharing sulfur atoms. In this way an average Mo−S coordination number of 6 would be achieved, in agreement with experimental evidence. Although it is possible to link these units together to yield an average oxidation state of +4 for molybdenum, it is impossible to produce a model containing all of the molybdenum in this oxidation state if units III and IV are included. Inspection of the "representative part of the MoS_3 structure" produced in the paper of Weber et al.[1] and simple bond counting reveal that Mo is in oxidation states ranging from 3 to 5. This contradicts their own claim that the structure is built entirely from Mo^{IV}-containing units. Jiao et al.[14] have modeled the structure of amorphous MoS_3 as isolated Mo_3S_9 units and taken the four cluster types of Weber et al.[1] as starting models for their computational studies using density functional theory. The energy-minimized Mo_3S_9 clusters of Jiao et al.[14] are shown in Figure 3, with structures III and IV being of lowest energy.

Although Jiao et al.[14] have attempted to retain a molybdenum oxidation state of 4, they make no comment on the fact that the initial and final models for the isolated clusters III and IV

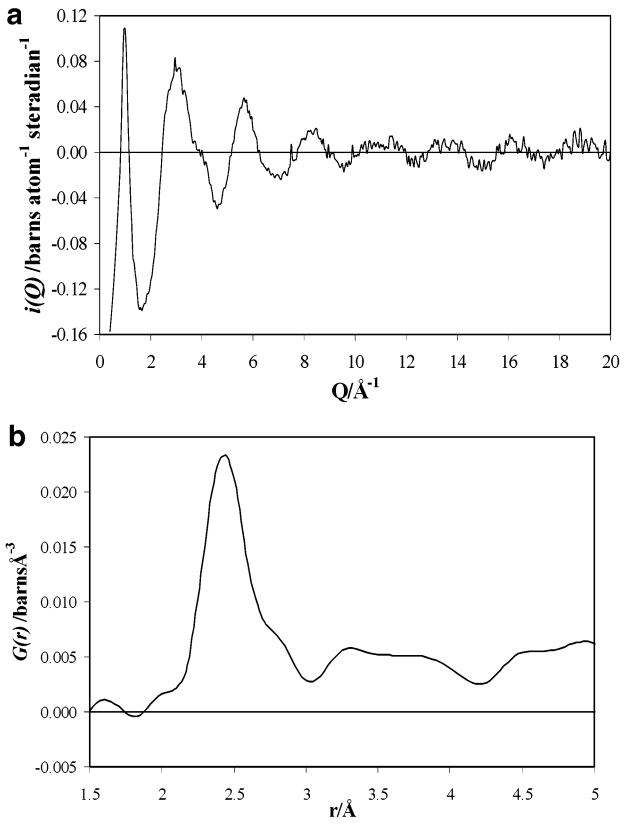

Figure 4. (a) Experimental interference function, $i_{exp}(Q)$, for MoS_3. (b) Experimental correlation function, $G_{exp}(r)$, for MoS_3.

contain molybdenum in different oxidation states and that their final minimized Mo_3S_9 clusters III and IV contain Mo in an average oxidation state of 4.67 $[(Mo^{4.67})_3(S^{2-})_5(S_2^{2-})_2]$.

The first requirement for all proposed structures is that they can account for the local structure. In this work we show that the isolated Mo_3S_9 cluster models proposed by Jiao et al.[14] do not even account for the experimentally determined function for MoS_3 over the 1.5−3 Å region. However, a realistic model must be able to do more than explain the local structure. It should also explain the correlation function at greater distances, the whole of the measured diffraction pattern and be able to be packed together to occupy three-dimensional space. We have used reverse Monte Carlo methods (RMC)[16] to construct large atomistic models for *a*-MoS_3, which fit the neutron diffraction data and are chemically realistic. Realistic structures must also be consistent with other experimental results. We discuss how our model might be reconciled with the experimental results of others and our own previous work. Finally we suggest further experiments to probe the structure of amorphous MoS_3.

Modeling

All models were tested against neutron diffraction data (Figure 4a), collected previously[10] using the LAD diffractometer[17] on the ISIS spallation neutron source at the Rutherford Appleton Laboratory.

(1) Models for MoS_3 Based on Isolated Mo_3S_9 Clusters. The experimental correlation function, $G_{exp}(r)$, for MoS_3 shown in Figure 4b is calculated from the interference function $i(Q)$,

(16) McGreevy, R. L.; Pusztai, L. *Mol. Simul.* **1988**, *1*, 359.
(17) Howells, W. S.; Soper, A. K.; Hannon, A. C. Rutherford Appleton Laboratory Report RAL-90-041; 1990; p 24.

Figure 4a, according to

$$G(r) = \frac{1}{2\pi^2 r}\int_0^{Q_{max}} Qi(Q)\, M(Q)\, \sin(Qr)\, dQ + g^o(\sum_l c_l \bar{b}_l)^2 \quad (1)$$

where $M(Q)$ is the Lorch modification function[18] (used to take into account that the diffraction pattern is measured up to a finite momentum transfer, Q_{max}, and not to infinity), g^o ($=N/V$) is the macroscopic atomic number density, c_l is the concentration of element l, and $\bar{b}_l$ is the corresponding neutron scattering length.

$$M(Q) = \frac{\sin(\pi Q/Q_{max})}{\pi Q/Q_{max}} \quad (2)$$

$G(r)$ is the sum of the weighted partial correlation functions:

$$G(r) = \sum_{m,n} c_m c_n \bar{b}_m \bar{b}_n g_{mn}(r) \quad (3)$$

where

$$g_{mn}(r) = \frac{n_{mn}(r)}{4\pi r^2\, dr} \quad (4)$$

and $n_{mn}(r)$ is the number of atoms of type n between r and $r + dr$ from an atom of type m. At low r it is sometimes possible to associate peaks in $G(r)$ with individual pair correlations. For example, the most prominent feature in $G_{exp}(r)$, Figure 4b, is the peak at about 2.5 Å corresponding to Mo−S correlations. The small peak around 2 Å corresponds to S−S correlations in S−S bonded units. The small area of this peak is due to the smaller number of such correlations and the small scattering length of sulfur ($\bar{b}_S = 0.2847 \times 10^{-14}$ m and $\bar{b}_{Mo} = 0.696 \times 10^{-14}$ m).[19] At higher r, contributions from different pair correlations sum together, and a simple interpretation of $G(r)$ is impossible. For example, the shoulder on the peak at 2.5 Å, which is at around 2.75 Å, is due in part to Mo−Mo correlation, but is also likely to contain contributions from S−S and possibly Mo−S correlations. In favorable cases, neutron diffraction experiments using different isotopes provide routes to obtaining individual pair correlation functions. However, the lack of a suitable isotope of sulfur precludes this approach in the case of MoS_3. An alternative approach is to build a model and to determine if $G_{calc}(r)$ is in agreement with $G_{exp}(r)$. We used this approach to test the models of Jiao et al.[14]

The correlation function, $G_{calc}(r)$, was calculated for each of Jiao et al.'s[14] models using the internuclear distances produced by their models to generate $i(Q)$ according to the Debye equation:[20]

$$i(Q) = \sum_m \sum_{n\neq m} \bar{b}_m \bar{b}_n \frac{\sin Qr_{mn}}{Qr_{mn}} \exp\left(\frac{-\langle u^2_{mn}\rangle Q^2}{2}\right) \quad (5)$$

where r_{mn} is the internuclear distance between the pair of atoms

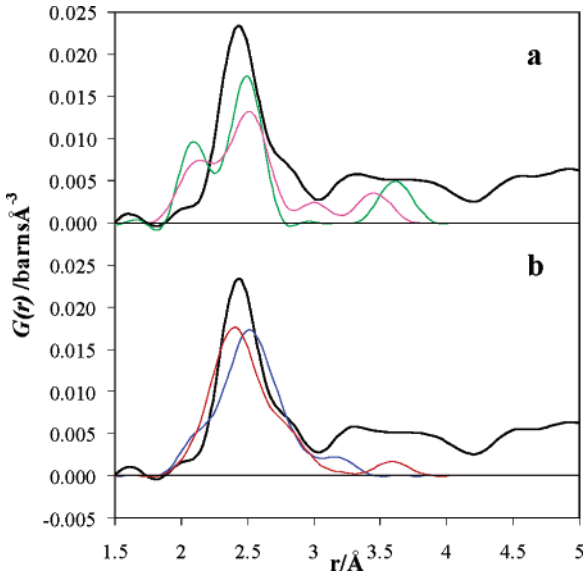

Figure 5. $G_{calc}(r)$ for the energy-minimized cluster models for MoS_3 of Jiao et al.[14] compared to $G_{exp}(r)$ (black line): (a) models I (green line) and II (pink line) and (b) models III (blue line) and IV (red line).

m and n, and $\langle u^2_{mn}\rangle$ is the estimated mean square variation in distance for this pair due to thermal broadening, and Fourier transforming this according to eq 1 after division by 9 to give $i(Q)$ for an average atom. Estimates of $\langle u^2_{mn}\rangle$ of $\langle u^2_{Mo-Mo}\rangle = 0.0036$ Å^2, $\langle u^2_{Mo-S}\rangle = 0.0026$ Å^2, and $\langle u^2_{S-S}\rangle = 0.0024$ Å^2 were obtained from a simple model, assuming harmonic motion and treating the atomic pairs as diatomic molecules with vibrational frequencies of 520, 380, and 210 cm^{-1} for for S−S, Mo−S, and Mo−Mo bonds, respectively.[21] This enabled us to compare directly $G_{exp}(r)$ with $G_{calc}(r)$ by including both the broadening effect of the finite Q_{max} used in our experimental work and thermal broadening in our model.

Comparison of $G_{exp}(r)$ and $G_{calc}(r)$, Figure 5, for the energy-minimized Mo_3S_9 clusters I and II of Jiao et al.[14] confirms their conclusion that these are poor models for the structure of amorphous MoS_3 over the 1.5−3 Å region. Not only does model I have an incorrect Mo−S coordination number, but the distribution of Mo−S bond lengths is also incorrect. The short terminal Mo═S bonds in this model, which produce the large peak in $G_{calc}(r)$ around 2.15 Å, are clearly not found in the real material. Model II presents similar problems, and neither model produces the shoulder at around 2.8 Å seen on the main peak in $G_{exp}(r)$.

Figure 5 shows that models III and IV of Jiao et al.,[14] although better than the first two models, are also inadequate in accounting for $G_{exp}(r)$. This is because the average Mo−S coordination number is still less than 6, being 5.67 and 5.33 for models III and IV, respectively, and the distribution of Mo−S bond distances is incorrect. Both models III and IV contain short terminal Mo═S bonds ($d_{Mo-S} = 2.13-2.15$ Å), which are not seen in $G_{exp}(r)$.

We believe that the approach of Jiao et al.,[14] in which isolated Mo_3S_9 clusters are used as models for amorphous MoS_3, cannot succeed, since MoS_3 is almost certainly an extended solid. In the past,[10] we have suggested that models based on the chain structure shown in Figure 1a could account for the local structure

(18) Lorch, E. A. *J. Phys. B* **1969**, *2*, 229.
(19) Sears, V. F. In *International Tables for Crystallography*; Kluwer Academic: Dordrecht, 1995; Vol. C, p 383.
(20) Wright, A. C. In *Experimental Techniques of Glass Science*; Simmons, C. J., El-Bayoumi, O. H., Eds.; The American Ceramic Society: Westerville, Ohio, 1993; Chapter 8, p 268.
(21) Teo, B. K. *EXAFS: Basic Principles and Data Analysis*; Springer-Verlag: Berlin, 1986; p 99.

determined in EXAFS[4−7] and neutron diffraction experiments.[10] We recently performed chemical excision experiments,[7] which, making the assumption that MoS_3 would react in the same way as isolated molybdenum sulfide clusters, suggested that about 70% of the molybdenum in MoS_3 is contained in Mo−Mo bonded triangles. This conclusion can also be reconciled with the local structure determined from neutron diffraction data[10] and with some of the EXAFS measurements.[4−7] However, we did not then attempt to produce space-filling models to test whether a realistic three-dimensional model could be constructed with this constraint imposed. Having considered and rejected the cluster models proposed by Jiao et al.[14] and the model of Weber et al.,[1] we decided to construct a large atomistic model for MoS_3 that was consistent with the experimental evidence. To achieve this, we have used reverse Monte Carlo (RMC) methods.[16]

(2) Large Atomistic Models for MoS_3. We used the reverse Monte Carlo program of McGreevy[16,22] to fit the interference function, $i_{exp}(Q)$, which we had obtained using neutron diffraction.[10] In RMC fitting, an initial configuration of atoms with the correct density is placed in the simulation box, and $i(Q)_{calc}$ is calculated from this atomic arrangement:

$$i(Q) = \int_0^\infty D(r)\frac{\sin Qr}{Q}\mathrm{d}r \tag{6}$$

where

$$D(r) = 4\pi r(G(r) - g^o(\sum_l \bar{b}_l)^2) \tag{7}$$

An atom is then moved at random and a new $i(Q)_{calc}$ is calculated. If the new configuration produces a better fit, measured by χ^2,

$$\chi_{i(Q)}{}^2 = \sum_{i=1}^{n}(i_{calc}(Q_i) - i_{exp}(Q_i))^2/\sigma(Q_i)^2 \tag{8}$$

where $\sigma(Q_i)$ is the experimental error (a single value of 0.0005 was used for each point in this work), the move is accepted. If the fit is worse, the move is accepted with a probability P, where

$$P = \exp(-(\chi_{new}{}^2 - \chi_{old}{}^2)/2) \tag{9}$$

This condition ensures that the fitting does not become stuck in local minima.

A recent review of the methodology and examples of applications can be found elsewhere.[23] The models produced by RMC are atomistic and contain information on partial pair correlation functions. Inspection of these functions provides an easy first check on whether a model is viable, before a more detailed consideration of the structural model. Because $i(Q)$ is the function fitted by RMC, $G(r)$ produced by summing the contributions made by $g_{MoMo}(r)$, $g_{MoS}(r)$, and $g_{SS}(r)$ is narrower than the corresponding function produced by Fourier transforming $i(Q)$, after a modification function has been employed to remove truncation ripples produced by the finite $Q_{max} = 20$ Å^{-1}. Real space comparisons with the experimental data are therefore made using the correlation function $G_{calc}(r)$ obtained by Fourier transforming $i_{calc}(Q)$ in an identical way to that used for the experimental data, with $Q_{max} = 20$ Å^{-1} and employing the Lorch function. In our modeling, we used configurations containing between 2880 and 6480 atoms and imposed global constraints on the closest approach of atoms in our final models of S- -S = 1.80 Å, Mo- -S = 2.30 Å, and Mo- -Mo = 2.60 Å. We used an atomic density of 0.0389 atoms/Å^3.

The constraints imposed by the observed density of a material and the closest approaches of atoms impose severe limitations on the possible structures that are consistent with the data. However, a large number of degrees of freedom still exists, and one of the general criticisms of RMC is that there are effectively too many variables refined for the available data. In this work, we have imposed very severe constraints by defining the connectivity of the models, and we use the RMC program to test if any of the proposed models are consistent with the experimental diffraction data. The RMC program can be run without diffraction data, but using constraints. This is a route to realistic starting models, which also greatly reduces the time required for the refinement to converge. We employed this technique in this work as described below.

MoS_3 Chain Models. A chain of composition MoS_3 and having the connectivity shown in Figure 1a was constructed by first considering only the molybdenum atoms. A spiral of five revolutions, containing 780 molybdenum atoms with alternating long and short Mo−Mo distances, was created. This chain spanned the length of the simulation box, with the two ends connected by the periodic boundary condition used in RMC. This single chain was then expanded to fill the box using the random moves of the RMC program, whilst retaining the connectivity of the molybdenum atoms. This resulted in the chain randomly tangling around itself as it spread into the box. The additional Mo−Mo constraints used were, d_{Mo-Mo} = 2.6−2.9 Å and d_{Mo-Mo} = 3.1−3.5 Å, for the short and long distance, respectively. Once this molybdenum framework was in place, three sulfur atoms were placed between every pair of molybdenum atoms, to provide the correct Mo−S connectivity for the model. Two types of sulfur atom were used to distinguish between the S^{-I} atoms, which form disulfides, and S^{-II} atoms, which do not form bonds to each other. The S^{-I} atoms were constrained to be connected to one other S^{-I} atom between 1.8 and 2.2 Å. The random moves of the program were then used again to move all the sulfur atoms to at least 2.6 Å away from all other sulfur atoms, except for those involved in the disulfide bond. A full listing of all the constraints used and of the final atomic coordinates for each model is available as Supporting Information. Two variations on the chain model were used, each containing different numbers of disulfide bonds: the $Mo^{IV}(S_2^{2-})(S^{2-})$ model and the $Mo^{V}(S_2^{2-})_{1/2}(S^{2-})_2$ model. In the $Mo^{V}(S_2^{2-})_{1/2}(S^{2-})_2$ model, there are disulfide groups bridging the Mo−Mo metal−metal bonded pairs, as shown in Figure 1a. In the $Mo^{IV}(S_2^{2-})(S^{2-})$ model, there are bridging disulfides between each pair of molybdenum atoms.

After the initial model had been constructed, the neutron diffraction data were introduced and the RMC program was run to produce the best fit to these data. Constraints were imposed to keep the $Mo^{V}(S^{2-})_2(S_2^{2-})_{1/2}$ chain intact, and the RMC program was run for about six million moves until the fit was oscillating about a χ^2 value of 59. Figure 6a shows the excellent final fit to $i(Q)$, Figure 6b the corresponding fit to $G(r)$, and Figure 6c the weighted contribution of the individual

(22) http://www.studsvik.uu.se.
(23) McGreevy, R. L. *J. Phys: Cond. Matter*. **2001**, *13*, R877.

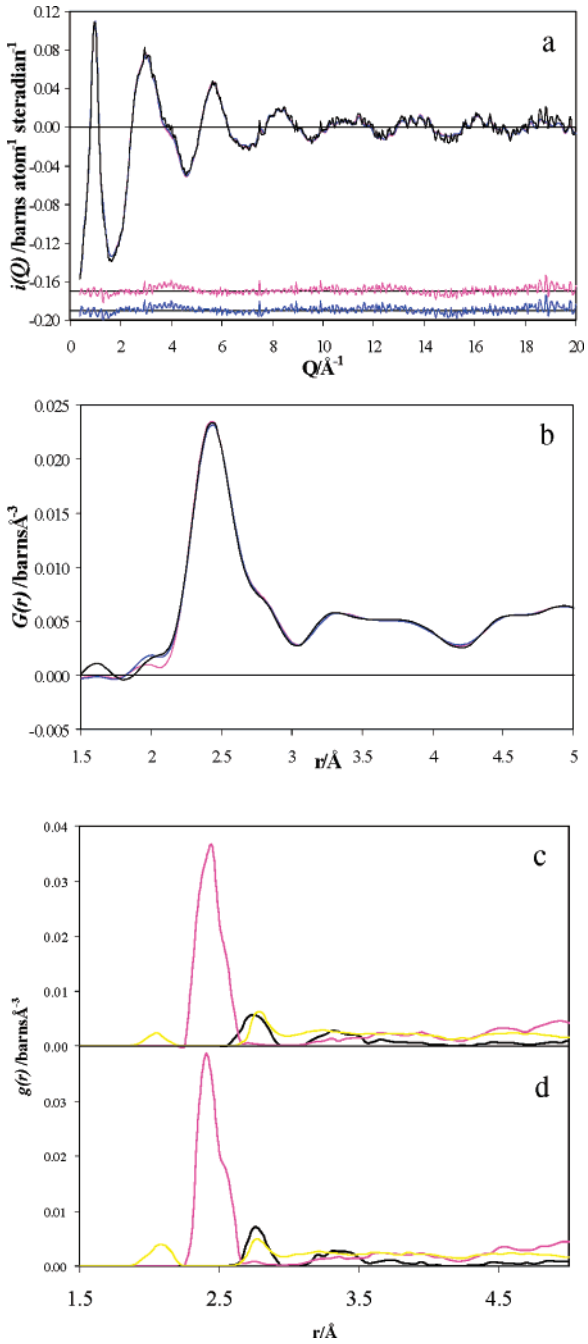

Figure 6. (a) RMC fit to $i_{exp}(Q)$ (black line) for the chain models, $i_{calc}(Q)$ Mo^{V} (pink line) and $i_{calc}(Q)$ Mo^{IV}(blue line). Difference plots are shown displaced by −0.17 and −0.19. (b) Comparison of $G_{exp}(r)$ (black line) and $G_{calc}(r)$ for the Mo^{V} (pink line) and Mo^{IV}(blue line) chain models. The neutron weighted partial $g(r)$'s from the RMC fitting for (c) Mo^{V} and (d) Mo^{IV} chain models ($g_{Mo-Mo}(r)$ (black line), $2g_{Mo-S}(r)$ (pink line), and $g_{S-S}(r)$ (yellow line)).

partial correlation functions for the model with the chemical formula $Mo^{V}(S^{2-})_2(S_2^{2-})_{1/2}$. Figures 6a, 6b, and 6c also show the results for the chain model with the formula $Mo^{IV}(S^{2-})(S_2^{2-})$ produced by introducing extra S−S bonds into the $(S^{2-})_3$ octahedral faces of the Mo^{V} model. This model also produced an excellent fit to $i(Q)$, with χ^2 oscillating around 57, and a better fit to $G(r)$ around 2 Å in the region of S−S correlations in the disulfide ion when compared to the $Mo^{V}(S^{2-})_2(S_2^{2-})_{1/2}$ chain models. Figures 7 and 8 show portions of two chain models after RMC fitting to the diffraction data.

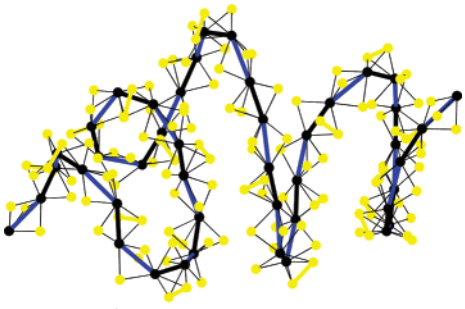

Figure 7. Portion of the $Mo^{V}(S^{2-})_2(S_2^{2-})_{1/2}$ chain model (solid circles Mo, yellow circles S, Mo−Mo bonds thick black line, and long nonbonded Mo−Mo distance blue line).

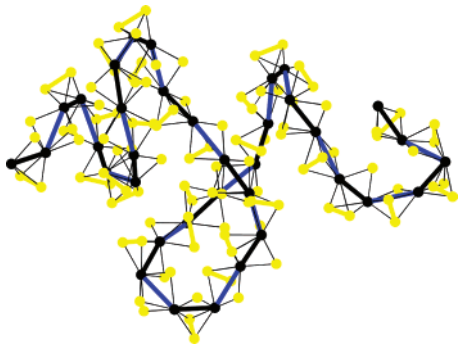

Figure 8. Portion of the $Mo^{IV}(S^{2-})_2(S_2^{2-})_{1/2}$ chain model (solid circles Mo, yellow circles S, Mo−Mo bonds thick black line, and long nonbonded Mo−Mo distance blue line).

MoS_3 Triangle Models. We have discussed above the impossibility of constructing models made from linked Mo_3S_{13} triangles and the difficulties in using the building blocks proposed by Weber et al.[1] to construct realistic extended structures. However, one of the units of Weber et al.,[1] I in Figure 2, can be linked with three similar units to produce a material containing all Mo atoms in oxidation state IV and with a Mo−S coordination number of 6. We constructed extended models composed of such units from carbon fullerenes, which have the correct connectivity with every carbon atom within the fullerene connected to three other carbon atoms. We derived our starting models from C_{80}, C_{240}, C_{320}, and C_{540}.[24] We replaced each carbon atom with a Mo_3 triangle centered at the position of the carbon atom to produce models containing 240, 720, 960, and 1620 Mo atoms. These triangles were then expanded into the simulation box using the random moves of the RMC program, whilst keeping the connectivity, until Mo−Mo bonded distances within the Mo_3 triangle were 2.6−2.9 Å and the Mo−Mo nonbonded distances to the next nearest molybdenum atoms were 3.1−4.0 Å. At this stage, the triangles appeared to be randomly spread around the box. The sulfur atoms were then added between the molybdenum atoms. It became apparent that the model derived from C_{80}, which contained 240 molybdenum atoms, was too rigid. The fits of the other triangle models to $i(Q)$ are shown Figure 9a and are significantly worse than those of the chain models, with χ^2 values of 77, 70, and 90 for the $(MoS_3)_{720}$, $(MoS_3)_{960}$, and $(MoS_3)_{1620}$ models, respectively. The fits are also worse in real space; Figure 9b shows $G_{calc}(r)$ compared to $G_{exp}(r)$. Furthermore the partial $g(r)$'s for the triangle models, Figure 9c, show unreasonably short S−S

(24) http://www.ccl.net/cca/data/fullerenes/index.shtml.

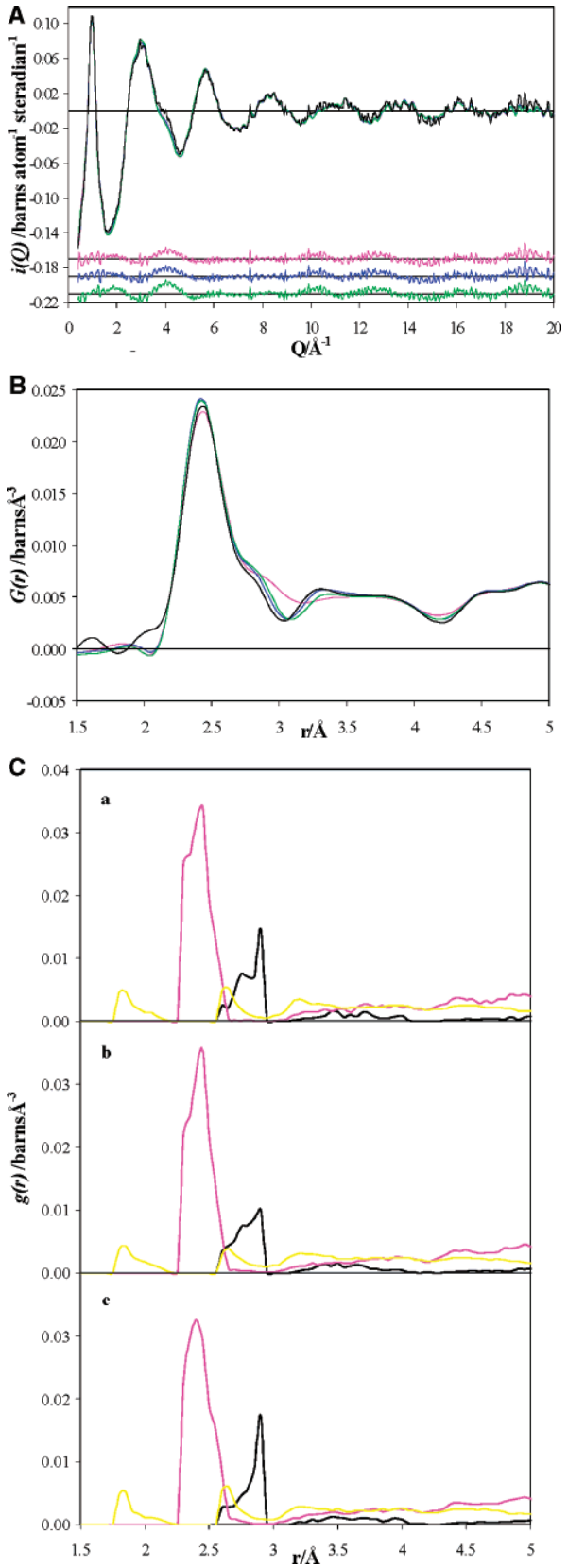

Figure 9. (A) RMC fit to $i_{exp}(Q)$ (black line) for the triangle models, $i_{calc}(Q)$ for $(MoS_3)_{720}$ (pink line), $(MoS_3)_{960}$ (blue line), and $(MoS_3)_{1620}$ (green line). Difference plots are shown displaced by −0.17, −0.19, and −0.21. (B) Comparison of $G_{calc}(r)$ for the $(MoS_3)_{720}$ (pink line), $(MoS_3)_{960}$ (blue line), and $(MoS_3)_{1620}$ (green line) triangle models with $G_{exp}(r)$ (black line). (C) Neutron-weighted partial $g(r)$'s from the RMC fitting of the $(MoS_3)_{720}$ (a), $(MoS_3)_{960}$ (b), and $(MoS_3)_{1620}$ (c) triangle models ($g_{Mo-Mo}(r)$ (black line), $2g_{Mo-S}(r)$ (pink line), and $g_{S-S}(r)$ (yellow line)).

contacts and physically unreasonable sharp cutoffs in $G(r)$ rather than a smoothly varying function.

Discussion

Our modeling shows that structural models of amorphous MoS_3, based on isolated Mo_3S_9 units, cannot account for the neutron data. Among other shortcomings, they have too low a Mo−S coordination number and incorrect Mo−S bond distances. We were not surprised by this result, since we and others believe that amorphous MoS_3 is likely to be an extended solid, and these models are also incompatible with EXAFS results.[4−7] In particular, no evidence is found in EXAFS experiments for the short terminal Mo═S bond found in these isolated Mo_3S_9 models. In the decomposition of $(NH_4)_2MoS_4$ to form MoS_3 the short Mo═S bond of 2.17 Å in the MoS_4^{2-} ion disappeared as MoS_3 was formed.[25]

We were initially surprised by how well the chain models fitted the neutron data when we constructed three-dimensional models using RMC. We had believed that chemical evidence supported the hypothesis that Mo_3 triangles were present in amorphous MoS_3. However, as we described above, there are problems with the construction of models for amorphous MoS_3 derived from Mo_3 triangular clusters. Although such models are initially attractive to chemists and can even explain most of the short-range structure, we can find no satisfactory way of linking these units together to account for the structural information from EXAFS and diffraction experiments. We have shown here that it is vital to consider whether proposed structural units can be linked together to form an extended solid that can occupy three-dimensional space and reproduce the diffraction pattern. We too have been guilty of this omission in the past in looking only at isolated units as models for amorphous MoS_3.

Can the chain structures for MoS_3, which account for the diffraction results, be reconciled with all the other experimental data? The chain model with the composition $Mo^{IV}(S_2^{2-})(S^{2-})$ is compatible with the photoelectron spectroscopy results of Weber et al.,[1] which show that all the Mo occurs as Mo^{IV} and that MoS_3 contains at least two types of sulfur. The S^{-I}/S^{-II} ratio is in agreement with the photoelectron spectroscopy results of Chianelli et al.,[4,8] if the chain has the composition $Mo^{V}(S^{2-})_2(S_2^{2-})_{1/2}$. Clearly, Weber at al.[1] and Chianelli et al.[4,8] are in disagreement here, but there are difficulties in determining oxidation states from PES measurements, and it would be worthwhile revisiting this problem. Another test is whether the chain models can account for the results from vibrational spectroscopy. We believe that they can. Our infrared data[6] and that of most other workers[1,4,11] show bands in the region 500−600 cm^{-1} that can be associated with S−S stretches. Only Weber et al.[1] observe a band at 460 cm^{-1}, which they assign to the Mo−S stretch of an apical sulfur bridging the face of a Mo_3 triangle. There is a difficulty in using the vibrational spectroscopy data of Weber et al.[1] to draw conclusions about the structural units present in MoS_3, in that the temperature at which these data were collected, 260 °C, is very close to the decomposition temperature of MoS_3, and it is likely that some MoS_2 is already forming. The appearance of the band at 460 cm^{-1} as MoS_2 is formed has been observed by others.[11] Considering all the available vibrational spectroscopy data, we believe they support the chain models. The most problematical

(25) Walton, R. I.; Dent, A. J.; Hibble, S. J. *Chem. Mater.* **1998**, *10*, 3737.

experimental results for proponents of the chain model are the results of chemical excision studies. Müller et al.,[12] Weber et al.,[1] and ourselves[7] have used chemical excision in an attempt to gain information on the structural units present in MoS_3. Reaction of MoS_3 with aqueous NH_3,[13] with HCl,[1] and with KCN[26,27] all produce triangular Mo_3 clusters. Weber et al.[1] used the information on the different species produced to estimate the number of each of the proposed structural units present in MoS_3, and on the basis that 35% of the molybdenum in MoS_3 was converted to $[Mo_3S_4(CN)_9]^{5-}$ on reaction with CN^- proposed that units III and IV made up 35% of the units in MoS_3. However, their conclusions were reached by measuring the yield of solid products only. In our recent quantitative work,[7] we found ~70% of Mo in MoS_3 was converted to $[Mo_3S_4(CN)_9]^{5-}$ in this reaction. Our results can only be reconciled with the chain structure of MoS_3 if the chain structure reacts to form Mo_3 clusters during chemical degradation. This reaction must occur rapidly because only Mo_3 clusters and Mo monomers were identified in our CN^- excision experiments, and the ratio of these species, 70% of Mo in Mo_3 clusters and 30% in monomeric species, did not change significantly with time. The elegant experiments of Müller et al.,[12] using a mixture of isotopically pure samples of $^{92}MoS_3$ and $^{100}MoS_3$ and reaction with OH^-, showed very little mixing of the two isotopes of molybdenum in their final Mo_3 cluster products. This also suggests that any reaction of the chain to form Mo_3 clusters must occur very rapidly, possibly on reaction if this is indeed the correct structure. It is tempting to suggest that the Mo_2 dimers in the chain might combine on reaction and eliminate a Mo monomer:

$$2\,Mo_2 = Mo_3 + Mo$$

This would predict that 75% of the molybdenum should appear in Mo_3 clusters on reaction with CN^-, in good agreement with the observed value.

Reviewing all the evidence on the structure of amorphous MoS_3, we believe that a jury would have to decide on the chain model rather than on a model based on Mo_3 triangles as providing the most likely explanation for the observations. However, to decide the case beyond doubt, further evidence should be gathered. The models we have constructed could be tested against further neutron and X-ray diffraction data. X-ray absorption and additional photoelectron spectroscopy experiments would be especially useful to quantify the amount of S^{-I} and S^{-II} and hence number of S−S bonds in MoS_3. This would allow discrimination between the two chain models for MoS_3 presented here. Further work on chemical excision on model molybdenum sulfide compounds would also be useful.

One lesson that should be drawn from our work here is that more must be taken into account when considering possible building blocks that might be present in an amorphous material than just the information available on short-range structure. Plausible structural models must fit the experimental results whilst occupying three-dimensional space with the correct density.

Conclusion

We have been able to construct a realistic three-dimensional chain model for the structure of MoS_3 using reverse Monte Carlo methods. Our model, formed from chains of MoS_6 octahedra sharing faces and with disulfides formed from pairs of sulfurs in the shared faces forming disulfide groups yielding the chemical formula $Mo^{IV}(S^{2-})(S_2^{2-})$, yields an excellent fit to the neutron diffraction data and can be reconciled with the other experimental evidence. We have also demonstrated that previously proposed models of amorphous MoS_3 based on isolated Mo_3S_9 are incompatible with neutron diffraction data and other experimental observations. Other models based on linking Mo_3 triangular clusters to form extended solids have been shown to be in disagreement with experimental results.

Acknowledgment. G.B.W. thanks the University of Reading for a studentship.

Supporting Information Available: Full listings of the constraints used to retain connectivity for the different models and atomic coordinates for the two chain models. This material is available free of charge via the Internet at http://pubs.acs.org.

JA037666O

(26) Müller, A. *Angew. Chem., Int. Ed. Engl.* **1980**, *19*, 72.
(27) Müller, A.; Krickmeyer, E.; Bögge, H.; Ratajczak, H.; Armatage, A. *Angew. Chem., Int. Ed. Engl.* **1994**, *33*, 770.